

AperTO - Archivio Istituzionale Open Access dell'Università di Torino

## Dynamical analysis of Microbial Fuel Cells based on planar and 3D-packed anodes.

### This is the author's manuscript

*Original Citation:*

*Availability:*

This version is available <http://hdl.handle.net/2318/1605242> since 2016-10-19T12:13:44Z

*Published version:*

DOI:10.1016/j.cej.2015.11.089

*Terms of use:*

Open Access

Anyone can freely access the full text of works made available as "Open Access". Works made available under a Creative Commons license can be used according to the terms and conditions of said license. Use of all other works requires consent of the right holder (author or publisher) if not exempted from copyright protection by the applicable law.

(Article begins on next page)

## Accepted Manuscript

Dynamical analysis of Microbial Fuel Cells based on planar and 3D-packed anodes

Tonia Tommasi, Adriano Sacco, Caterina Armato, Diana Hidalgo, Livio Millone, Alessandro Sanginario, Elena Tresso, Tiziana Schilirò, Fabrizio C. Pirri

PII: S1385-8947(15)01641-1  
DOI: <http://dx.doi.org/10.1016/j.cej.2015.11.089>  
Reference: CEJ 14487

To appear in: *Chemical Engineering Journal*

Received Date: 20 August 2015  
Revised Date: 24 November 2015  
Accepted Date: 25 November 2015



Please cite this article as: T. Tommasi, A. Sacco, C. Armato, D. Hidalgo, L. Millone, A. Sanginario, E. Tresso, T. Schilirò, F.C. Pirri, Dynamical analysis of Microbial Fuel Cells based on planar and 3D-packed anodes, *Chemical Engineering Journal* (2015), doi: <http://dx.doi.org/10.1016/j.cej.2015.11.089>

This is a PDF file of an unedited manuscript that has been accepted for publication. As a service to our customers we are providing this early version of the manuscript. The manuscript will undergo copyediting, typesetting, and review of the resulting proof before it is published in its final form. Please note that during the production process errors may be discovered which could affect the content, and all legal disclaimers that apply to the journal pertain.

# Dynamical analysis of Microbial Fuel Cells based on planar and 3D-packed anodes

Tonia Tommasi<sup>1,\*</sup>, Adriano Sacco<sup>1</sup>, Caterina Armato<sup>1,3</sup>, Diana Hidalgo<sup>1,2</sup>, Livio Millone<sup>2</sup>,  
Alessandro Sanginario<sup>1</sup>, Elena Tresso<sup>1,2</sup>, Tiziana Schilirò<sup>3</sup>, Fabrizio C. Pirri<sup>1,2</sup>

<sup>1</sup> Center for Space Human Robotics @Polito, Istituto Italiano di Tecnologia,  
Corso Trento 21, 10129, Torino, Italy.

<sup>2</sup> Department of Applied Science and Technology (DISAT), Politecnico di Torino,  
Corso Duca degli Abruzzi 24, 10129, Torino, Italy.

<sup>3</sup> Department of Public Health and Pediatrics, University of Torino,  
Piazza Polonia 94, 10126, Torino, Italy.

\* Corresponding author: [tonia.tommasi@iit.it](mailto:tonia.tommasi@iit.it), tel. +39.011.5091953, fax. +39.011. 5091 901

## Abstract

The aim of this paper is to provide a real time monitoring of the performances of microbial fuel cells (MFCs) employing two different anode configurations with a mixed consortia coming from seawater: a planar structure, constituted by carbon felt, and an innovative 3D-packed structure, constituted by graphitized Berl saddles. A detailed exam of the dynamical behavior of the two cells is presented in order to analyze the differences between planar and 3D-packed structures. Both the bacteria communities composition and MFCs electrical properties have been monitored over 31 days. The effects on the cell performances of the start-up phase, of the feeding operation and of an external applied resistance are discussed. The energy losses inside the MFCs along time, before and after refill of chemical solutions have been obtained by means of electrochemical impedance spectroscopy. Results show that after 10 days of operations the total internal resistances decreased of about 30% and

50% for carbon felt and graphitized saddles anodes, respectively. The reduction of internal resistances is in agreement with improved performance in terms of power density. Moreover, for both MFCs the refill operation leads to a reduction of the impedances, in particular the anodic resistances decreases while the ohmic and the cathodic ones are quite unaffected. In addition, the energy production of the two devices was studied applying resistive loads for 10 days. The saddle-MFC presents more stable voltage values if compared to the other cell, implying a larger energy production over time. Finally, Quantitative real-time Polymerase Chain Reaction analysis, performed over the whole period of investigation on planktonic phase, reveals the presence of two typical electrogens bacteria, such as *Geobacter* and *Shewanella*.

**Keywords:** Bioconversion; Biofilms; Bioprocess Monitoring; Packed Bed Bioreactors; Microbial Fuel Cell; Electrochemical Impedance Spectroscopy.

## 1. Introduction

A microbial fuel cell (MFC) is a bioelectrochemical system constituted by an anode and a cathode for the direct conversion of chemical energy into electricity by simultaneously treating organic waste. In the anode chamber, the decomposition of organic substrates by microbes via the respiration chain generates electrons ( $e^-$ ) and protons ( $H^+$ ) that are transferred to the cathode through an external electric circuit and a cation exchange membrane (CEM), respectively [1]. MFCs do not require traditional fuel supply, as common fuel cells; moreover they do not need to be recharged/replaced after exhaustion, as it happens for lithium ion batteries. However, due to theoretical and practical limitations, they are not yet suitable for high energy demands. Their optimal application is foreseen for

powering sensors and communication systems either in harsh environments or remote terrestrial areas [2–6].

Involving both electrochemical processes and microbiology aspects, the overall performance of an MFC depends on a variety of factors, such as materials design, bacteria involved and operative conditions [7–10]. A significant parameter that reflects the performances of MFCs is the internal resistance  $R_{\text{int}}$  [11–15] (including anode resistance, cathode resistance, electrolyte resistance, and membrane resistance), which limits the output power [1]. Its value depends on MFC design and operation parameters such as substrate concentration, pH, temperature and ionic strength of the electrolyte and, also, it varies during the microbial activities. Moreover, the internal resistance strongly depends on the intrinsic characteristics of the employed materials and it can be reduced by increasing the surface area of the anode [16], of the cathode [17] and of the membrane [18]. The identification of the factors limiting the conversion efficiency of an MFC requires to quantify the contribution of each component to the total internal resistance, taking into account the energy losses during the evolving of the process, that are mainly due to mass transfer, ohmic and activation losses [19–23]. Electrochemical Impedance Spectroscopy (EIS) has been proposed as a good tool for the comprehension of the dynamic evolution of the MFC system [24]. The final performance of an MFC is decisively related to the density of electrochemically active bacteria that can grow at the anode and by the rate of electron transfer from the bacteria to the electrode. For this reason the choice of the electrode materials, their configuration and operative conditions play a fundamental role in an MFC design.

The electrodes must generally exhibit good electric conductivity, adequate chemical stability, high mechanical strength and possibly low cost. In addition, specific requirements are needed for the electrode in contact with bacteria: high surface roughness, excellent

biocompatibility, high surface area and good porosity, efficient electron transfer between bacteria and electrode surface [25]. Carbon-based materials are generally preferred because of their good biocompatibility, good chemical stability, high conductivity and relatively low cost [25–29]. Moreover three dimensional architectures offer advantages such as to improve porous electrode structures, to increase the surface area and to obtain better biofilm growth and substrate propagation conditions. Reticulated vitreous carbon or graphite felt [30] have been used in small mini-MFCs as efficient 3D-electrodes; open-pore carbon foam, employed both as anode and cathode, has exhibited good stability and fair robustness [31]; highly conductive brush anodes in graphite fibers have been largely employed in tubular, bottle and cube shaped reactors [32]. The coverage of stainless steel fiber nanofelts with carbon nanoparticles such as graphene, carbon nanotubes and activated carbon has shown to be an effective method for high performant anodes [33]. Open celled carbon scaffolds have been obtained by carbonizing the microcellular polyacrylonitrile (PAN) and PAN/graphite composites with supercritical CO<sub>2</sub> as foaming agent [34] and hydroxylated and aminated polyaniline nanowire networks were synthesized and used as MFC anodes to enhance the electrical outputs [35]. Finally, more recently, in view of obtaining cost-effective and environmental friendly electrodes, natural and “green” nanostructured 3D materials have been suggested. They range from wood-based biochar made using forestry residue with pore size in the range 10-60 Å [36], to lightweight hollow fibers made by kapok plants [37] to the kenaf stems, a byproduct of the crop that via a simple carbonization procedure are used to obtain a conducting electrode with an ordered macroporous architecture [38]. It has however to be noted that for the majority of these novel electrodes [30–38] the time-dependent performances and the scaling-up possibilities of the production methods have not yet been reported. Moreover the comparison with

results obtainable using traditional planar electrodes is missing. So, further research is needed to confirm the effectiveness in view of future applications.

Depending on their configuration, the MFCs electrodes can be divided in planar, packed structures or brush structures [32]. Examples of planar structures are: carbon paper and mesh, graphite plates or sheets and carbon cloth or felt, even if some materials, e.g. carbon felt or mesh have a higher specific surface area [26,28,39–41]. Packed-structures are becoming increasingly common in MFCs [13,42–45] since they provide high surface area available to bacteria. In fact, as for the biological filter for wastewater treatment, the anode chamber of the MFC can be filled with granular or irregular shaped packing scaffolds in order to have high concentration of microorganisms per unit of volume.

The main challenge for MFC technology is to replace the energy-expensive aerobic wastewater treatment approach (such as activated sludge and aerobic biofilm processes) with low-energy consumption ones [46]. For biofilm reactors, such as fixed and fluidized beds reactors, plastic or ceramic materials fabricated in grains with different shapes and dimensions are often selected. However, the granular packing material must be conductive to be used in MFC (e.g. granular graphite and active carbon [47–49]). In order to make the complete bed conductive, the granules must be tightly packed next to each other, although dead zones for current collection may still exist after long term running [32]. To this end, packed granules are often used in MFCs experiments [50] even if the problem of biofouling can occur: granules are heavy and could clog [32].

In this work an original solution for packed carbon-based electrodes is employed [51], through the graphitization of the so-called Berl saddles. Berl saddles constitute a packed support for bacteria, traditionally used in immobilized bed reactor, either in anaerobic or aerobic conditions, where there is a presence of gas phase. They are often employed in

vacuum distillation, absorption and extraction because they provide high useable contact surface area ( $1150 \text{ m}^2/\text{m}^3$ ) with high void bed fraction (about 80%); moreover, they can sustain high temperatures (till  $1100^\circ\text{C}$ ), they are cheap and easily commercially available. These items are electrically insulating ceramic supports of length of about 6 mm with the shape of a saddle “without inside and outside faces” [52]; they can be made electrically conductive by a convenient graphitization procedure [43]. When graphitized Berl saddles are employed in the anode of MFC, where anaerobic conditions are present, the gas produced by bacteria metabolisms can easily migrate out of the system, due to the high bed void fraction, avoiding the increase of pressure in the anode chamber. In addition, Berl saddles can help to reduce biofouling and at the same time favor the growth of biofilm.

The graphitized-Berl saddles have already been characterized from a structural point of view, with *Saccaromyces cerevisiae* and external electron mediator (methylene blue) [51]. The aim of this paper is to study the dynamics of an MFC system, comparing, over a period of 31 days, two different anode-configurations: a planar one (carbon felt) and a 3D-packed granular structure (graphitized Berl saddles). A mixed population coming from seawater (without the addition of external mediators) has been used. Marine water has been chosen as inoculum because is a complex high-conductivity, geochemical active ecosystem of major importance in the global carbon cycle [53]. The two MFCs were fed at fixed days, their voltages were online-monitored and their polarization curves were acquired at alternate days. After stabilization of the open circuit potential (about 21 days), external resistances were applied to the cells for the last 10 days of the test, and the energy production was measured. During the whole period of investigation, impedance spectroscopy (EIS) and real-time quantitative Polymerase Chain Reaction (RT-qPCR) analyses were carried out. The obtained results are discussed in correlation with electrical performances of the MFCs,



focusing on the different behaviour of planar and 3D-packed structures. We demonstrate that the graphitized Berl saddles open a new possibility for designing cost-effective and easy-manufacturing anodes, very promising for large-scale practical applications.

## **2. Experimental**

### **2.1 MFCs design and operation**

Two identical MFCs were designed: each one is based on two circular chambers, namely the anode and the cathode. Both compartments were made in Poly(methyl methacrylate) (PMMA) with internal diameter and thickness of 12 and 1.5 cm respectively (internal volume for each chamber  $\sim 170$  mL) separated by a cation exchange membrane (CEM, CMI 7000, Membranes International Inc., Glen Rock, NJ, USA). A carbon felt (Soft felt SIGRATHERM GFA5, SGL Carbon, Germany) was used in one of the MFC as a planar anode electrode and assembled together with a graphite rod (diameter 5 mm, SGL Carbon, Germany) to ensure an effective current conduction capability. In the second MFC, carbon-coated Berl saddles were used to obtain a granular packing electrode, assembled together with a graphite rod in order to collect electrons. The procedure followed for obtaining the carbon-coated Berl saddles is described in paragraph 2.2, while a deep electrochemical and morphological characterization is reported in our recent work [51]. Both MFCs were inoculated in the anode chambers by sea water, previously enriched with following cultures (in five steps) in anaerobic conditions as described in the paragraph 2.3. A carbon sheet (Carolina, USA) joined with a graphite rod was used as cathode electrode in both MFCs. We performed the experiments at room temperature ( $24 \pm 2$  °C). The first 21 days of tests have been conducted in Open Circuit condition, in order to have the adaptation of bacteria to the new conditions inside the MFC and to permit electrode colonization. After the start-up period,

MFCs operated under external resistance applied between anode and cathode chamber. Each MFC was running in semi-continuous mode (fed-batch) using a Syringe Pump (NE-1600 Programmable Syringe Pump, USA) with Hydraulic Retention Time (HRT) of 6.5 days for each reactor, feeding a synthetic substrate at pH 7, with the following organic carbonaceous loading rate in g/L for a day: 1  $\text{C}_6\text{H}_{12}\text{O}_6$ , 1  $\text{CH}_3\text{CO}_2\text{Na}$  and 1.25 peptone. The cathode compartment was filled by potassium ferricyanide (6.58 g/L) used as oxidant compound, and solution of mineral salts (8.2 g/L of  $\text{Na}_2\text{HPO}_4$  and 5.2 g/L of  $\text{NaH}_2\text{PO}_4$ ) was used as a buffer in both anode and cathode chamber. These reagents were dissolved in 75% v/v filtered sea water and 25% v/v distilled water. The mixing of the solutions at both anode and cathode chambers was obtained by recirculating anolyte and catholyte with a 500 mL reservoir by using multichannel peristaltic pumps at both anode and cathode chambers (Peri-Star Pro 4 and 8 channel, USA, respectively), with a flow rate of 30 mL/min. The schematic view and a picture of set-up are shown in Figure 1a and b, respectively.

## 2.2 Preparation of the packed anode

$\alpha$ -D-glucose was used to deposit a conductive carbon layer on the porcelain Berl saddles (Product cod. Z169013 Sigma Aldrich, Germany). The Berl saddles were firstly accurately cleaned in ultrasonic bath for 10 min at 1.8 kW using ethanol to remove pollutants from the surface and then dried in air at room temperature. Subsequently, the Berl saddles (250 g) were immersed in 200 mL of glucose solution (500 g/L) in distilled water under gently stirring conditions for 24 h. The Berl saddles were then separated by filtration from the glucose solution and caramelized at 185°C under vacuum for 24 h. The caramelized material was pyrolyzed at 800 °C under Argon flow (500 mL/min) in a horizontal tube furnace for 2 h (heating rate of 5 °C/min), and then let cooling down overnight.

### 2.3 Bacterial growth conditions

The inoculum chosen come from seawater (Arma di Taggia (IM), Italy). It has been taken from the interface between water and atmosphere and it contains high number of diverse planktonic populations, where extracellular enzymes produced by the resident population degrade organic matter naturally present in seawater, transferring electrons. The seawater sample was inoculated into anodic chamber of MFC after an enrichment procedure. In fact, the fresh seawater sample, before the use inside the anode as inoculum, was previously enriched in 250 mL glass flasks in three following steps. In the first step, the fresh seawater was inoculated (10% v/v) into a synthetic substrate, with the following composition in g/L: 7 C<sub>6</sub>H<sub>12</sub>O<sub>6</sub>, 8.2Na<sub>2</sub>HPO<sub>4</sub>, 5.2 NaH<sub>2</sub>PO<sub>4</sub>, 8 CH<sub>3</sub>CO<sub>2</sub>Na, 7 fructose and 10 peptone. These reagents were dissolved in 75% v/v filtered sea water and 25 % v/v distilled water. After that, the pH of the culture was set-up in the range 7 - 7.5 by adding NaOH 2 M. Furthermore, in order to reach strictly anaerobic condition, the culture was purged by high-speed N<sub>2</sub> flow for 5 min. The medium used for bacteria growth is general and few selective to allow growing of resident marine consortia in order to have a high biodiversity in the inoculum. The enriched culture was grown at room temperature (24 ± 2 °C) and under gentle orbital shaking (150 rpm). The bacteria growth was monitored as a function of the time by measuring the optical density (OD) at 600 nm. When OD was inside the range 0.5 - 0.8 (i.e. inside the range of the exponential phase of bacteria growth), 10% culture was used as inoculum of a new fresh culture (second step), using the same medium and the same operative conditions described before. Once the culture reached again an OD value in the range 0.5 - 0.8, it was inoculated in the third fresh medium, repeating the same procedure. Finally, when OD was again in the

range 0.5 - 0.8, the bacteria suspension was ready to be inoculated into the MFCs, with a ratio of 10% v/v of the total anode volume.

## 2.4 Characterization techniques and instrumentation

The morphology of both carbon felt and carbon-coated Berl saddles (before and after the carbon layer deposition) was evaluated through Field Emission Scanning Electron Microscopy (FESEM, ZEISS Dual Beam Auriga). The resistivity measurements on the two different anode materials were carried out using a Keithley 2635 Source Measure Unit in four-point probe configuration. During the first 21 days of operation both cells were maintained in open circuit voltage (OCV) configuration, and their potential was continuously monitored by using a Data Acquisition Unit (Agilent, 34972A). During this period, the performances of the cells were analyzed through different electrochemical techniques: Linear Sweep Voltammetry (LSV), Current Interrupt (CI) method and Electrochemical Impedance Spectroscopy (EIS). All these experiments were carried by a multi-channel VSP potentiostat (BioLogic) in a two-electrode set-up configuration: a working electrode was coupled to the anode and both counter and reference electrode were connected to the cathode, respectively); the data were recorded by using EC-Lab<sup>®</sup> software version 10.1x (BioLogic). Polarization curves were obtained by LSV using a scan rate of 1 mV/s. The CI method was carried out using a perturbation to the system with a very short duration (50 ms): when the MFC produced a stable current output ( $I$ ) at fixed potential (0.30 V), the circuit was opened, thus causing an initial steep potential ( $V_R$ ) rise followed by a further slow increase of the potential ( $V_A$ ). The steep increase is referred to as the ohmic losses expressed as ohmic resistance ( $R_\Omega$ ), which can be calculated as  $R_\Omega = V_R / I$  [54]. Impedance

spectroscopy measurements were carried out in two-electrode configuration at cell open circuit voltage, exploiting an AC signal with amplitude equal to 10 mV and frequency range 100 mHz – 20 kHz. The experimental data were fitted through the equivalent circuit reported in Fig. 2 [24]. Each electrode is modeled through a polarization resistance ( $R_{an}$  and  $R_{cat}$  for anode and cathode, respectively) and a constant phase element (CPE) associated to the double layer ( $Q_{an}$  and  $Q_{cat}$  for anode and cathode, respectively), while the series resistance  $R_s$  takes into account the ohmic losses due to cables, electrolyte and membrane. In the anodic compartment, the Warburg impedance  $Z_w$  is associated to diffusion limitations. For all the investigation period, anode and cathode solutions were refilled thrice a week. Before and after the refill procedure, all the electrochemical measurements were repeated, in order to check the effect of the solution depletion.

After the start-up phase ended (21 days), the performances of the fuel cells were evaluated by applying a load between the electrodes, and calculating the generated power output for a period of 10 days. The current production during stabilized operation of fuel cells was monitored by connecting them to various external resistances (100, 330, 560, 680, 820 and 1000  $\Omega$ ) and measuring the voltage through a Data Acquisition Unit (Agilent, 34972A).

## 2.5 RT-qPCR analysis

In order to identify and quantify some bacterial communities involved in anaerobic respiration leading to the production of electricity in an MFC, Real Time quantitative Polymerase Chain Reaction (RT-qPCR) analysis were performed in planktonic liquid phase for the following genera of microorganisms: Total Bacteria, Total Sulfate Reducing Bacteria (SRB) and Total Sulfate Oxidating Bacteria (SOB), *Acetobacter*, *Clostridium*, *Geobacter*, *Saccharomyces*, *Shewanella*. These microorganisms were chosen as markers of the phylum

Proteobacteria ( $\alpha$ - Proteobacteria: *Acetobacter*;  $\gamma$ -Proteobacteria: *Geobacter* and  $\delta$ -Proteobacteria: *Shewanella*), Firmicutes (*Clostridium*) and Ascomycota (*Saccharomyces*). Genomic DNA was extracted with a commercial kit (UltraClean™ Microbial DNA Isolation Kit, MO-BIO Laboratories Inc., Carlsbad, CA) according to manufacturer's instructions. Gene target and primers were selected by the international scientific literature (**Table I**). The RT-qPCR used a standard super-mix (Bio-Rad SsoFast\_EvaGreen SuperMix) for each strain and a standard power-mix (Bio-Rad IQ™ Multiplex PowerMix) for Total Bacteria. Opticon Monitor 3 Software and the RT-qPCR Chromo4 (Bio-Rad) were used to perform and analyze the RT-qPCR. Optimal thermal cycling parameters consisted of an initial 3.5 min denaturation step at 95 °C followed by 40 cycles at 95 °C for 30 s, 55 °C for 45 s and 72 °C for 30 s. After every RT-qPCR, except for Total Bacteria, a melting curve was run with the following thermal conditions: from 55 °C to 95 °C read every 0.5 °C, and read plate at 95 °C.

## 2.6 Statistics

Statistical analyses were performed with the SPSS Package version 21.0 for Windows. Student's t-test was applied to compare two groups of independent samples. The differences were considered significant at  $p < 0.05$ .

## 3. Results and discussion

### 3.1 Material properties

Carbon felt was used as anode electrode first of all because it exhibits high mechanical strength, good conductivity and high surface area ( $1.5 \text{ g/m}^2$ ); furthermore, its planar structure reduces the distance between the two electrodes improving MFC performance [64]. Carbon felt photograph and FESEM images are shown in Figures 3a, 3b and 3c. FESEM images evidence that the material is constituted by cylindrical carbon fibers randomly

arranged: this fact makes it a suitable place for bacterial growth. Figure 3d shows the carbon-coated Berl saddles used as anode electrode in the second MFC. From Raman characterization reported in [51], the presence of conductive graphitic and amorphous carbon was observed. As evidenced by FESEM images shown in Figures 3e and 3f, the graphitized saddles exhibit a very rough surface that can promote the adhesion and the growth of the bacteria. The carbon-coating obtained after deposition process of glucose on the pristine Berl saddles (specific surface area of  $1.5 \text{ m}^2/\text{g}$ ) results homogeneous with thickness of about  $7 - 8 \text{ }\mu\text{m}$  (as shown in the inset of Figure 3e). In addition, the structure of the graphitized Berl saddles provides a high useable contact surface area with high void bed fraction ( $1115 \text{ m}^2/\text{m}^3$ ), useful to avoid an increase of pressure in the anode chamber caused by gas production during the activity of microorganisms. The electrical properties of the materials were evaluated in four-point probe configuration, obtaining for the carbon felt a resistivity of about  $(35 \pm 10) \text{ m}\Omega/\text{cm}^2$  and for one isolated Berl saddle a value of  $(50 \pm 10) \Omega$ .

### 3.2 Start-up and dynamic evolution

The evolution of OCV, maximum power density ( $P_{\text{max}}$ ) and internal resistance ( $R_s$ ,  $R_a$ ,  $R_c$ ) over time was studied through electrical and electrochemical tests. At the very beginning, the uncolonized anodes were inactive. Then, in the first period (21 days of operation) the acclimatization of bacteria at the new conditions inside MFCs occurs, and hence the cell potentials at open circuit conditions were rapidly increasing, passing from values of 0.2 and 0.45 V for graphitized saddles and carbon felt, respectively, to stable potentials equal to 0.7 V for both type of cells. This feature indicates a successful startup; in fact the planktonic microbial population in the anode chamber of both MFCs slightly decreases probably as a consequence of anode colonization as well (Figures 4a and 4b). After that period, both the

MFCs show an increase of the performances as reported in the polarization curves at 10 and 17 days (Figure 5a). The polarization curve of carbon felt shows a point of maximum power (MPP) greater than graphitized saddle after start-up (the corresponding current densities at MPP are  $1.17 \text{ A/m}^2$  and  $0.23 \text{ A/m}^2$ , respectively). However, the very rapid drop of voltage visible from LSV (Figure 5a) without a substantial increase of the current, and the correspondent power densities curve (Figure 5b) with a visible and sharp peak, show an unstable MPP for carbon felt-based electrodes. On the contrary, graphitized saddles permit to have more stable conditions moving around MPP voltage (Figure 5). It has to be noted that LSV evaluation gives a ready-reference of the behavior of the electrical parameters (voltage, current and power) for both planar and packed electrodes. However, in biological systems such as MFCs, more truthful information is obtained by monitoring the system under external loads, as it will be shown in paragraph 3.6. Accordingly to LSV curves, the internal resistances of both cells decreased of about 14% between initial time and 10-days operating conditions. This reduction can be explained by the growth of anode-reducing microorganisms which colonize the electrodes but it can also be due to the bulk solution creating a biofilm on carbon felt surface and around the Berl saddles. This improves the electron transport mechanisms between cell membrane and anode and hence reduces the internal resistance (which limits the current output). According to RT-qPCR, *Geobacter* and *Clostridium*, for carbon felt MFC, and *Acetobacter*, for Berl saddles MFC, show a pattern that could account for colonization, even if the quantitative decrease is not statistically significant (Figure 4). Comparing the results obtained by planar and 3D-packed materials, the first one (i.e. carbon felt) gives the best performances in terms of maximal output power density ( $P_{\max}$ ), reaching after 10 days the value of about  $227 \text{ mW/m}^2$  against the value of  $77 \text{ mW/m}^2$  obtained with the 3D-packed material (Berl saddles). Taking into account that the



ratio between the geometrical anode surface and the total volume of the anodic chamber is  $655 \text{ cm}^2/\text{L}$ ,  $P_{\text{max}}$  values turn out to be about  $15 \text{ mW/L}$  for carbon felt and  $5 \text{ mW/L}$  for graphitized Berl saddles anodes, respectively. It has to be noted that the  $P_{\text{max}}$  values obtained with 3D-packed materials are lower than with planar material, and also lower with respect to other researches on mixed population [65–67] and on 3D electrodes [31,32,35,36]. In the power density curves (Figure 5b) sharp peaks are observed for the carbon felt MFC. This fact indicates the risk of instability under real operation conditions, when the systems work either at fixed current or at fixed voltage. On the contrary, Graphitized Saddles-MFC evidence stable MPP conditions over a wide range of voltage values. In fact, the high bed void fraction (80%) created by Berl saddles packaging provides an open 3D space accessible to microbial growth which permits a long-operation and an effective electron transfer from the bacteria to the anode. Recently, granules and biofilm-based system have been widely used since they are capable of maintaining higher biomass concentration and could operate at higher dilution rate without biomass washout, permitting a reduction of the reactor volume [68]. We verified that during the time of the test no clogging of the electrode as consequence of gas entrapment occurred, thus confirming the possibility of using these innovative graphitized Berl saddles as anode in MFCs also for scale-up purposes.

### 3.3 Microbes in anodic chambers and their role

Rt-qPCR analyses conducted on the planktonic microorganisms revealed that in the anolytes of both MFCs, mainly *sulfate-oxidizing* and *sulfate-reducing bacteria* (SOB and SRB) and bacteria belonging to the Proteobacteria phylum (*Geobacter* and *Shewanella*) were grown. In addition, Firmicutes (*Clostridium*) and Ascomycota (*Saccharomyces*) phyla were detected

in small percentages (Figure 4). In particular, in the carbon felt anode a slight decrease of *Shewanella* concentration values (and, as a consequence, of the total bacteria) was detected after 17 days, while the values remained quite constant in the Berl saddles-based anode (Fig. 4a and 4b, respectively). Nakagawa et al. [69] reported that *Shewanella oneidensis* MR-1 acquires the ability to utilize glucose after an initial exposure to glucose, as in our case of microorganism exposure in a pre-culture medium beyond the feeding. In general, members of the *Shewanella* genus have great flexibility in terms of growth strategy and metabolisms [70], allowing them to proliferate in diverse and changing environments. It was interesting to detect along the time-course of the experiments, the presence of *Geobacter* in both planktonic phases, even if many studies reported the presence of *Geobacter* only on the anodic biofilm because of their principal electron transfer mechanisms [71]; however other studies reported that *Geobacter* is also able to produce electron shuttles as mechanism for the extracellular electron transfer in the mixed consortium[72]. Similarly to this study, also Lee et al. [73] found *Geobacter* sp. in MFC fed with a mixture of glucose and acetate. The presence of *Geobacteriaceae* spp. guarantees an electron transfer to the electrode that is mediated both by extracellular conductive biological nanowires (pili), also at long-range (on the order of 1 cm), and by redox proteins, which are c-cytochromes present in the external membrane of bacterium [62,74]. Beyond the direct transfer mechanisms (like *Geobacteriaceae* spp.), *Shewanellariaceae* spp. possess the possibility to excrete soluble flavin redox molecules as natural electron shuttles. Even if these bacteria constitute only about 3% of the total population, their concentration is relatively abundant considering that they include a sole species within the wide diversity of microorganisms living in seawater, involved in many ecophysiological processes (e.g. nitrogen, sulfur, iron and phosphorous cycling). Based on bacteria and electrical properties of MFCs, a higher concentration of

bacteria (especially if electroactive), favors a stable electricity generation, as was observed from the polarization curves after some days of acclimations (Figure 5). With RT-qPCR analysis we identified only ~25% of planktonic component of the anode chambers; in particular tables in Figure 4 evidence that SOB and SRB are the most abundant (~20%) with respect to total bacteria in both case (there are no significant difference between the two MFCs anodic component as confirmed by t-test,  $p>0.05$ ). This reflects the environment condition of the chosen inoculum: sulfate is abundant in sea water and SRB are widely distributed in anoxic marine sediments, as members of microbial communities, and at hydrothermal vents [53]. Although most marine bacteria and Archea can assimilate sulfate for biosynthesis of cellular compounds, SRB have the ability to link the oxidation of substrates to adenosine triphosphate (ATP) generation, using sulfate as electron acceptor. While SRB are found in several phyla of the bacteria, the most important types are member of the *δ-proteobacteria*, and their activities are highly significant in the sulfur cycle in anoxic marine environments, where they utilize organic compound or hydrogen as electron donors [53]. The big variety of bacteria could be attributed to the “poor selective” anaerobic enrichment procedure, which contains different carbon sources (acetate, glucose and fructose) and therefore can promote distinct metabolisms and bacteria. This choice was made in order to see how the marine resident population can electrochemically behave inside MFC. In fact, taking advantages from living-cells, MFC can be used in natural environment (e.g. seawater) as biological sensors or to power electronics/commercial sensors for environment parameters monitoring directly into the sea. In our case, even if *Geobacter* nor *Shewanella* grow fermentatively, other bacteria have fermentative metabolisms, such as *Clostridium*, that produce acetate, electrons and protons starting from glucose. Therefore, acetate in its turn is used for other species, as *Geobacter* or *Shewanella*,

showing how is important the “bacteria-cooperation” in natural environment. Moreover, another kind of “cooperation” in natural environment regards the electrons transfer gained from the carbon sources to the electrode from plankton to the electrode: if the mediators are produced in considerable quantities, other bacteria could use them as electron shuttles [75,76].

### 3.4 Electrochemical Impedance Spectroscopy analysis

The obtained LSV results (Figure 5) were successfully confirmed by EIS analysis for both types of cells, as reported in Figure 6a. As expected from the polarization data, the impedance values for the carbon felt-MFC are lower with respect to the graphitized Berl saddles one. In view of a quantitative evaluation of the internal MFC resistances, the experimental data were fitted through the equivalent circuit reported in Figure 2, and the fitted curves are reported in Figure 6a superimposed to the measured spectra. As it can be clearly seen, a good match was obtained, meaning an effective choice of the equivalent circuit [24,77]. The resistance values extracted from the fitting procedures are reported in Table II. By comparing these values, a significant difference in the anodic resistances of the two cells can be noted, while series and cathodic ones present similar values. It is worthy to note that the effect of such a high  $R_{an}$  is responsible for the masking of the Warburg feature in the impedance plot of the saddles-based MFC. As evident in Figure 6a, the low frequency straight line that is clearly visible in the felt-based MFC (associated with the diffusion), is not observable in the other cell spectrum (for this reason the  $Z_w$  value is not reported for this cell in Table II). Different reasons can contribute to the larger anode impedances observed for saddles-based MFCs. First of all, the intrinsic lower conductivity of the graphitized Berl saddles with respect to the felt (as reported in Section 3.1). In addition, in the case of Berl

saddles, the particular 3D-packed structure is capable to kept also dead bacteria adhered to the anode material, while in the case of felt-based cells only live biofilm tends to remain attached on the surface. The presence of such non-active layer can likely inhibit to a certain extent the effective charge transfer in the anodic compartment of saddle-based MFCs. The impedance measurements were repeated for all the period of investigation, and they always present similar characteristic for both MFCs (data not shown). However, a slight decrease of the series and cathode resistances occurred after 10 days of operation for both type of cells. The anode resistances experienced the largest reduction: in the case of Berl saddles-based MFC, after 10 days its value is lower than the half of the initial one, while for the felt-based cell the reduction is of 30%. This decrease has a positive effect in the current density production, in accordance to the polarization curves of Figure 5, and it is compatible with the biofilm growth. Finally, the series resistance values, calculated from the EIS analysis, do not match the exact values calculated from the CI method, even if they qualitatively agree. This is a well known issue for the current interrupt method, since MFCs are bio-electrochemical systems in which the polarization resistance associated with the microbial activity is not negligible if compared to the ohmic one. As a consequence, the CI method (essentially based on the Ohm's law) is not able to accurately evaluate the internal resistance [77]. This result confirms once more that EIS technique is a powerful tool for an accurate analysis of the MFCs behavior.

Starting from the fitting of the EIS spectra collected all over the start-up period under open circuit condition, the characteristic time constant of each electrode was calculated exploiting the following formula [78]:

$$\tau = (RQ)^{1/\beta}$$

where  $R$  and  $Q$  represent the resistance and the CPE related to one electrode (i.e. anode or cathode) and  $\theta$  is the CPE index. The calculated values as a function of the time are reported in Figure 6b. It can be observed a sensible decrease of the anode characteristic time  $\tau_{an}$  for both types of cells: about one order of magnitude for the graphitized Berl saddles and more than two orders for the carbon felt anode. This behavior is in perfect agreement with the already observed enhancement of the cell performances due to the improved properties of the anodic biofilm over time. Moreover, in accordance to the previous discussed measurements, also in this case the carbon felt-based cell exhibits better performances, as evidenced by the lower  $\tau_{an}$  values, meaning a faster charge transfer mechanism. On the other hand, quite stable values were observed for the cathodic characteristic times, since the counter electrode performances are not affected by the biofilm growth. In addition, as expected, these values are practically identical for the two MFCs, being the cathodic compartments equal for the two different cells.

### 3.5 Feeding operation

In order to assess the effectiveness of the feeding operation, LSV measurements were carried out before and 1 h after the replacement of fresh organic substrate media and cathode solution, when the power generation returned to a steady value. As shown in Figures 7a and 7b for the Berl saddles cell, the good maintenance of fresh reagents in both chambers results extremely important, even if anolyte and catholyte recirculation was continuously guaranteed and the operating conditions, such as substrate concentration and pH were maintained constant. Figure 7a shows for example that the short circuit current density ( $J_{sc}$ ) in MFC with Berl saddles increases of about 2 times after refill (reaching 0.39 A/m<sup>2</sup>), and OCV goes from 0.59 V to 0.73 V. The huge increase of current is due to the

reactivation of bacteria metabolisms after *famine* conditions for the depletion of the fuel (which is mainly glucose, acetate and peptone), with the consequent releasing of electrons to the anode electrode. Consequently, also the power output (Figure 7b) increases, reaching 85 mW/m<sup>2</sup>. Vice versa, the increase in the voltage is mainly attributable to the refill of catholyte, as demonstrated from cathode polarization curves before and after refill (data not shown).

Also EIS analysis was carried out before and after the feeding operation. The measured spectra and the corresponding fitting curve (obtained through the equivalent circuit of Fig. 2) are reported as an example in Figure 7c for the Bell saddles cell. For both types of cell, the refill operation reflects a reduction of the measured impedances, meaning that the inlet of fresh media is effective in reducing the charge transfer resistances, in agreement with previously reported results [79,80]. From the analysis of the cell parameters obtained from the fitting procedure (reported in Table III) it can be seen that the feeding operation leads to a decrease of the anodic resistances while the ohmic and the cathodic ones are quite unaffected. These findings are of particular interest in the field of MFCs, because they open the way for EIS as a tool that can be exploited for the monitoring of cell faults under continuous operation conditions. In fact, on-line impedance measurements make possible the observation of physical effects like the glucose concentration decreasing, as in this case, by monitoring the dynamic evolution of the cell performances.

### 3.6 Investigation of MFCs under external load

Even if MFC with carbon felt gives the highest power density as measured by LSV (see for example Figure 5), it is well known in the literature that this kind of measurement does not completely reflect the real behavior of the cell when a load is applied between its electrodes

[81]. For this reason, the voltage output of both kinds of cell was monitored along time while applying different resistors. In Figure 8 the potential and the calculated power are reported together with the applied resistance values. As visible in the graphs, both MFCs show similar voltage values, even if the saddle-based MFC seems having more stable voltage values, resisting better in correspondence of nutrients depletion (Figure 8). The explanation of this behavior resides on the better filling of the conductive electrode, niches and “anchorage” for bacteria within anodic chamber, that facilitate electron transfer from bacteria to the electrode, both in direct and indirect way, by contact or endogenous electron transfer, respectively. In accordance with the above reported consideration, the energy productions of the cells under resistances (calculated by integrating the output power over time) were found to be 355 and 376 J for carbon felt and graphitized saddles, respectively. Finally, by comparing Figures 5 and 8, it is worthy to note that the responses of the cells to a voltage slope equal to 1 mV/s by LSV bring to performances which are one order of magnitude higher than under external resistances, showing that LSV slightly overestimates the current production and therefore the obtainable power density.

#### 4. Conclusions

The electrode configuration plays an important role on the dynamics of microbial fuel cells. In this work, we presented a study on two different anode materials: a carbon felt (with a planar structure) and a random network of graphitized Berl saddles (with a 3D-packed structure). A detailed exam of the dynamical behavior of the two cells was performed by monitoring the evolution of both the bacteria communities composition and electrical properties of MFCs over a time interval of 31 days. The different electrochemical behaviors



were studied through impedance spectroscopy. This technique has proven to be a very useful tool for monitoring the onset of MFC faults, when performed on-line under continuous operation conditions. The results obtained for commercial carbon felt and graphitized Berl saddle are comparable for the obtained electrical performances as well as for the investigated population established in the anodic chamber. However the graphitized saddles open a new possibility for designing cost-effective and easy-manufacturing anodes, promising for large-scale practical applications. In fact, this strategy allows obtaining, by an easy procedure, a good packing material for bacteria growth and proliferation, which helps in reducing biofouling and exhibits low electrical resistance for the direct recovery of electrons by bacteria metabolisms. In addition, the efficient nutrients and gas diffusion permits to obtain a biofilm reactor with good recovery of electricity, towards an energy-sustainable wastewater treatment plant realization.

### **Acknowledgements**

The authors are most grateful to Valentina Cauda, Angelica Chiodoni, Katarzyna Bejtka (Istituto Italiano di Tecnologia) and Samuele Porro (Politecnico di Torino), for their important contribution on the material synthesis and characterization. Furthermore, the authors thanks to Prof. Bernardo Ruggeri (Politecnico di Torino) for his valuable scientific contribution.

**Bibliography**

- [1] B.E. Logan, B. Hamelers, R. Rozendal, U. Schröder, J. Keller, S. Freguia, et al., Microbial fuel cells: methodology and technology, *Environmental Science & Technology*. 40 (2006) 5181–5192.
- [2] B.E. Logan, Scaling up microbial fuel cells, *Appl Microbio Biotechnol*. 85 (2010) 1665–1671.
- [3] S. Cheng, B.E. Logan, Increasing power generation for scaling up single-chamber air cathode microbial fuel cells, *Bioresource Technology*. 102 (2011) 4468–4473.
- [4] B. Jong, B. Kim, I. Cheng, L. PWY, Y. Choo, G. Kang, Enrichment performance and microbial diversity of a thermophilic mediatorless microbial fuel cell, *Environmental Science & Technology*. 40 (2006) 6449–6454.
- [5] H. Ren, H. Lee, J. Chae, Miniaturizing microbial fuel cells for potential portable power sources: promises and challenges, *Microfluid Nanofluid*. 13 (2012) 353–381.
- [6] T. Tommasi, A. Chiolerio, M. Crepaldi, D. Demarchi, A microbial fuel cell powering an all-digital piezoresistive wireless sensor system, *Microsystem Technologies*. 20 (2014) 1023–1033.
- [7] I.T. Vargas, I.U. Albert, J.M. Regan, Spatial distribution of bacterial communities on volumetric and planar anodes in single-chamber air-cathode microbial fuel cells., *Biotechnology and Bioengineering*. 110 (2013) 3059–62.
- [8] C.I. Torres, A. Kato Marcus, B.E. Rittmann, Proton transport inside the biofilm limits electrical current generation by anode-respiring bacteria., *Biotechnology and Bioengineering*. 100 (2008) 872–81.
- [9] T. Krieg, A. Sydow, U. Schröder, J. Schrader, D. Holtmann, Reactor concepts for bioelectrochemical syntheses and energy conversion., *Trends in Biotechnology*. 32 (2014) 645–55.
- [10] X. Quan, Y. Quan, K. Tao, Effect of anode aeration on the performance and microbial community of an air-cathode microbial fuel cell, *Chemical Engineering Journal*. 210 (2012) 150–156.
- [11] A.K. Manohar, F. Mansfeld, The internal resistance of a microbial fuel cell and its dependence on cell design and operating conditions, *Electrochimica Acta*. 54 (2009) 1664–1670.
- [12] Z. He, S.D. Minteer, L.T. Angenent, Electricity generation from artificial wastewater using an upflow microbial fuel cell, *Environmental Science & Technology*. 39 (2005) 5262–7.

- [13] K. Rabaey, P. Clauwaert, P. Aelterman, W. Verstraete, Tubular microbial fuel cells for efficient electricity generation, *Environmental Science & Technology*. 39 (2005) 8077–82.
- [14] D. Hidalgo, A. Sacco, S. Hernández, T. Tommasi, Electrochemical and impedance characterization of Microbial Fuel Cells based on 2D and 3D anodic electrodes working with seawater microorganisms under continuous operation., *Bioresource Technology*. 195 (2015) 139–146.
- [15] J.C. Biffinger, R. Ray, B.J. Little, L. a Fitzgerald, M. Ribbens, S.E. Finkel, et al., Simultaneous analysis of physiological and electrical output changes in an operating microbial fuel cell with *Shewanella oneidensis*., *Biotechnology and Bioengineering*. 103 (2009) 524–531.
- [16] V. Watson, G. Estadt, Graphite Fiber Brush Anodes for Increased Power Production in Air-Cathode Microbial Fuel Cells, *Environ. Sci. Technol.* 41 (2007) 3341–3346.
- [17] S. Oh, B. Min, B.E. Logan, Cathode performance as a factor in electricity generation in microbial fuel cells, *Environmental Science & Technology*. 38 (2004) 4900–4904.
- [18] S.-E. Oh, B.E. Logan, Proton exchange membrane and electrode surface areas as factors that affect power generation in microbial fuel cells, *Applied Microbiology and Biotechnology*. 70 (2006) 162–169.
- [19] H. Wang, J.-D. Park, Z. Ren, Active energy harvesting from microbial fuel cells at the maximum power point without using resistors., *Environmental Science & Technology*. 46 (2012) 5247–52.
- [20] J.C. Biffinger, J. Pietron, O. Bretschger, L.J. Nadeau, G.R. Johnson, C.C. Williams, et al., The influence of acidity on microbial fuel cells containing *Shewanella oneidensis*, *Biosensors & Bioelectronics*. 24 (2008) 906–911.
- [21] S. Cheng, D. Xing, B.E. Logan, Electricity generation of single-chamber microbial fuel cells at low temperatures, *Biosensors & Bioelectronics*. 26 (2011) 1913–1917.
- [22] H. Liu, S. Cheng, B.E. Logan, Production of electricity from acetate or butyrate using a single-chamber microbial fuel cell, *Environmental Science & Technology*. 39 (2005) 658–662.
- [23] Z. He, Y. Huang, A.K. Manohar, F. Mansfeld, Effect of electrolyte pH on the rate of the anodic and cathodic reactions in an air-cathode microbial fuel cell, *Bioelectrochemistry*. 74 (2008) 78–82.
- [24] X. Dominguez-Benetton, S. Sevda, K. Vanbroekhoven, D. Pant, The accurate use of impedance analysis for the study of microbial electrochemical systems, *Chemical Society Reviews*. 41 (2012) 7228–7246.

- [25] J. Wei, P. Liang, X. Huang, Recent progress in electrodes for microbial fuel cells, *Bioresource Technology*. 102 (2011) 9335–9344.
- [26] X. Wang, S. Cheng, Use of Carbon Mesh Anodes and the Effect of Different Pretreatment Methods on Power Production in Microbial Fuel Cells, *Environ. Sci. Technol.* 43 (2009) 6870–6874.
- [27] I. Ieropoulos, J. Greenman, C. Melhuish, Microbial fuel cells based on carbon veil electrodes: Stack configuration and scalability, *International Journal of Energy Research*. (2008).
- [28] Q. Deng, X. Li, J. Zuo, A. Ling, B.E. Logan, Power generation using an activated carbon fiber felt cathode in an upflow microbial fuel cell, *Journal of Power Sources*. 195 (2010) 1130–1135.
- [29] Y. Feng, Q. Yang, X. Wang, B.E. Logan, Treatment of carbon fiber brush anodes for improving power generation in air – cathode microbial fuel cells, *Journal of Power Sources*. 195 (2010) 1841–1844.
- [30] E. Henderson, P.K. Wu, J. Pietron, R. Ray, B. Little, J.C. Biffinger, High Power Density from a Miniature Microbial Fuel Cell Using *Shewanella oneidensis* DSP10, *Environmental Science & Technology*. (2006) 2629–2634.
- [31] G. Lepage, F.O. Albernaz, G. Perrier, G. Merlin, Characterization of a microbial fuel cell with reticulated carbon foam electrodes., *Bioresource Technology*. 124 (2012) 199–207.
- [32] B. Logan, S. Cheng, V. Watson, G. Estadt, Graphite fiber brush anodes for increased power production in air-cathode microbial fuel cells, *Environmental Science & Technology*. 41 (2007) 3341–6.
- [33] J. Hou, Z. Liu, S. Yang, Y. Zhou, Three-dimensional macroporous anodes based on stainless steel fiber felt for high-performance microbial fuel cells, *Journal of Power Sources*. 258 (2014) 204–209.
- [34] Y. Wang, H. Huang, B. Li, W. Li, Novelty developed three-dimensional carbon scaffold anodes from polyacrylonitrile for microbial, *Journal of Materials Chemistry A: Materials for Energy and Sustainability*. 3 (2015) 5110–5118.
- [35] Y. Zhao, S. Nakanishi, K. Watanabe, K. Hashimoto, Hydroxylated and aminated polyaniline nanowire networks for improving anode performance in microbial fuel cells., *Journal of Bioscience and Bioengineering*. 112 (2011) 63–6.
- [36] T. Huggins, H. Wang, J. Kearns, P. Jenkins, Z. Jason, Biochar as a sustainable electrode material for electricity production in microbial fuel cells, *Bioresource Technology*. 157 (2014) 114–119.

- [37] H. Zhu, H. Wang, Y. Li, W. Bao, Z. Fang, C. Preston, et al., Lightweight , conductive hollow fi bers from nature as sustainable electrode materials for microbial energy harvesting, *Nano Energy*. 10 (2014) 268–276.
- [38] S. Chen, G. He, X. Hu, M. Xie, S. Wang, D. Zeng, et al., A three-dimensionally ordered macroporous carbon derived from a natural resource as anode for microbial bioelectrochemical systems., *ChemSusChem*. 5 (2012) 1059–63.
- [39] S. Cheng, B.E. Logan, Ammonia treatment of carbon cloth anodes to enhance power generation of microbial fuel cells, *Electrochemistry Communications*. 9 (2007) 492–496.
- [40] Y. Liu, F. Harnisch, K. Fricke, U. Schröder, V. Climent, J.M. Feliu, The study of electrochemically active microbial biofilms on different carbon-based anode materials in microbial fuel cells, *Biosensors and Bioelectronics*. 25 (2010) 2167–2171.
- [41] A. Morozan, L. Stamatina, F. Nastase, A. Dumitru, S. Vulpe, C. Nastase, The biocompatibility microorganisms-carbon nanostructures for applications in microbial fuel cells, *Pyhsica Status Solidi (a)*. 204 (2007) 1797–1803.
- [42] M. Di Lorenzo, K. Scott, T.P. Curtis, I.M. Head, Effect of increasing anode surface area on the performance of a single chamber microbial fuel cell, *Chemical Engineering Journal*. 156 (2010) 40–48.
- [43] P. Aelterman, M. Versichele, M. Marzorati, N. Boon, W. Verstraete, Loading rate and external resistance control the electricity generation of microbial fuel cells with different three-dimensional anodes, *Bioresource Technology*. 99 (2008) 8895–902.
- [44] P.R. Bandyopadhyay, D.P. Thivierge, F.M. McNeilly, A. Fredette, An Electronic Circuit for Trickle Charge Harvesting From Littoral Microbial Fuel Cells, *IEEE Journal of Oceanic Engineering*. 38 (2013) 32–42.
- [45] F. Li, Y. Sharma, Y. Lei, B. Li, Q. Zhou, Microbial fuel cells: the effects of configurations, electrolyte solutions, and electrode materials on power generation, *Applied Biochemistry and Biotechnology*. 160 (2010) 168–81.
- [46] S.T. Oh, J. Rae, G.C. Premier, T. Ho, C. Kim, W.T. Sloan, Sustainable wastewater treatment: How might microbial fuel cells contribute, *Biotechnology Advances*. 28 (2010) 871–881.
- [47] D. Jiang, B. Li, Granular activated carbon single-chamber microbial fuel cells ( GAC-SCMFCs ): A design suitable for large-scale wastewater treatment processes, *Biochemical Engineering Journal*. 47 (2009) 31–37.
- [48] S. You, Q. Zhao, J. Zhang, J. Jiang, A graphite-granule membrane-less tubular air-cathode microbial fuel cell for power generation under continuously operational conditions, *Journal of Power Sources*. 173 (2007) 172–177.

- [49] B. Erable, N. Duteanu, S.M.S. Kumar, Y. Feng, M.M. Grangrekar, K. Scott, Nitric acid activation of graphite granules to increase the performance of the non-catalyzed oxygen reduction reaction ( ORR ) for MFC applications, *Electrochemistry Communications*. 11 (2009) 1547–1549.
- [50] M. Di Lorenzo, T.P. Curtis, I.M. Head, K. Scott, A single-chamber microbial fuel cell as a biosensor for wastewaters, *Water Research*. 43 (2009) 3145–3154.
- [51] D. Hidalgo, T. Tommasi, V. Cauda, S. Porro, A. Chiodoni, K. Bejtka, et al., Streamlining of commercial Berl saddles : A new material to improve the performance of microbial fuel cells, *Energy*. 71 (2014) 615–623.
- [52] Sigma Aldrich,  
<http://www.sigmaaldrich.com/catalog/product/aldrich/z169013?lang=it&region=IT>, (Last access: June 2015).
- [53] C. Munn, *Marine Microbiology- Ecology and Application*, Second Edi, Garland Science, New York and London, 2011.
- [54] P. Aelterman, K. Rabaey, H. The Pham, N. Boon, W. Verstraete, Continuous electricity generation at high voltages and currents using stacked microbial fuel cells, *Communications in Agricultural and Applied Biological Sciences*. 71 (2006) 63–6.
- [55] W. Xu, Z. Huang, X. Zhang, Q. Li, Z. Lu, J. Shi, et al., Monitoring the microbial community during solid-state acetic acid fermentation of Zhenjiang aromatic vinegar., *Food Microbiology*. 28 (2011) 1175–81.
- [56] B. Dridi, M. Henry, A. El Khéchine, D. Raoult, M. Drancourt, High prevalence of *Methanobrevibacter smithii* and *Methanosphaera stadtmanae* detected in the human gut using an improved DNA detection protocol., *PloS One*. 4 (2009) e7063.
- [57] Q. Xia, T. Williams, D. Hustead, P. Price, M. Morrison, Z. Yu, Quantitative analysis of intestinal bacterial populations from term infants fed formula supplemented with fructo-oligosaccharides., *Journal of Pediatric Gastroenterology and Nutrition*. 55 (2012) 314–20.
- [58] D.E. Cummings, O.L. Snoeyenbos-West, D.T. Newby, a. M. Niggemyer, D.R. Lovley, L. a. Achenbach, et al., Diversity of geobacteraceae species inhabiting metal-polluted freshwater lake sediments ascertained by 16S rDNA analyses, *Microbial Ecology*. 46 (2003) 257–269.
- [59] D.W. Himmelheber, S.H. Thomas, F.E. Löffler, M. Tallefert, J.B. Hughes, Microbial Colonization of an In Situ Sediment Cap and Correlation to Stratified Redox Zones, *Environmental Science & Technology*. 43 (2009) 66–74.
- [60] B. Meyer, J. Kuever, Molecular analysis of the diversity of sulfate-reducing and sulfur-oxidizing prokaryotes in the environment, using *aprA* as functional marker gene., *Applied and Environmental Microbiology*. 73 (2007) 7664–79.

- [61] B. Meyer, J. Kuever, Phylogeny of the alpha and beta subunits of the dissimilatory adenosine-5'-phosphosulfate (APS) reductase from sulfate-reducing prokaryotes--origin and evolution of the dissimilatory sulfate-reduction pathway., *Microbiology (Reading, England)*. 153 (2007) 2026–44.
- [62] S. Bensaid, B. Ruggeri, G. Saracco, Development of a Photosynthetic Microbial Electrochemical Cell (PMEC) Reactor Coupled with Dark Fermentation of Organic Wastes: Medium Term Perspectives, *Energies*. 8 (2015) 399–429.
- [63] S. A. Dar, L. Yao, U. van Dongen, J.G. Kuenen, G. Muyzer, Analysis of diversity and activity of sulfate-reducing bacterial communities in sulfidogenic bioreactors using 16S rRNA and *dsrB* genes as molecular markers., *Applied and Environmental Microbiology*. 73 (2007) 594–604.
- [64] M. Zhou, M. Chi, J. Luo, H. He, T. Jin, An overview of electrode materials in microbial fuel cells, *Journal of Power Sources*. 196 (2011) 4427–4435.
- [65] T.H. Pham, P. Aelterman, W. Verstraete, Bioanode performance in bioelectrochemical systems: recent improvements and prospects, *Trends Biotechnol.* 27 (2009) 168–178.
- [66] X. Xie, L. Hu, M. Pasta, G.F. Wells, D. Kong, C.S. Criddle, et al., Three-Dimensional Carbon Nanotube - Textile Anode for High-Performance Microbial Fuel Cells, *Nano Letters*. 11 (2011) 291–296.
- [67] B. Cercado, L.F. Cházaro-Ruiz, V. Ruiz, I.D.J. López-Prieto, G. Buitrón, E. Razo-Flores, Biotic and abiotic characterization of bioanodes formed on oxidized carbon electrodes as a basis to predict their performance., *Biosensors & Bioelectronics*. 50 (2013) 373–381.
- [68] Z.-P. Zhang, S.S. Adav, K.-Y. Show, J.-H. Tay, D.T. Liang, D.-J. Lee, et al., Characteristics of rapidly formed hydrogen-producing granules and biofilms., *Biotechnology and Bioengineering*. 101 (2008) 926–36.
- [69] G. Nakagawa, A. Kouzuma, A. Hirose, T. Kasai, G. Yoshida, K. Watanabe, Metabolic Characteristics of a Glucose-Utilizing *Shewanella oneidensis* Strain Grown under Electrode-Respiring Conditions., *PloS One*. 10 (2015) 1–14.
- [70] Y.J. Tang, R. Chakraborty, H.G. Martín, J. Chu, T.C. Hazen, J.D. Keasling, Flux analysis of central metabolic pathways in *Geobacter metallireducens* during reduction of soluble Fe(III)-nitrilotriacetic acid., *Applied and Environmental Microbiology*. 73 (2007) 3859–64.
- [71] E. Marsili, D.B. Baron, I.D. Shikhare, D. Coursolle, J. a Gralnick, D.R. Bond, *Shewanella* secretes flavins that mediate extracellular electron transfer., *Proceedings of the National Academy of Sciences of the United States of America*. 105 (2008) 3968–73.

- [72] K. Rabaey, N. Boon, S.D. Siciliano, M. Verhaege, W. Verstraete, Biofuel cells select for microbial consortia that self-mediate electron transfer., *Applied and Environmental Microbiology*. 70 (2004) 5373–82.
- [73] Y.-Y. Lee, T.G. Kim, K.-S. Cho, Effects of proton exchange membrane on the performance and microbial community composition of air-cathode microbial fuel cells., *Journal of Biotechnology*. 211 (2015) 130–7.
- [74] D. Sanchez-Herrera, D. Pacheco-Catalan, R. Valdez-Ojeda, B. Canto-Canche, X. Dominguez-Benetton, J. Domínguez-Maldonado, et al., Characterization of anode and anolyte community growth and the impact of impedance in a microbial fuel cell., *BMC Biotechnology*. 14 (2014) 102.
- [75] M.E. Hernandez, A. Kappler, D.K. Newman, Phenazines and Other Redox-Active Antibiotics Promote Microbial Mineral Reduction, *Applied and Environmental Microbiology*. 70 (2004) 921–928.
- [76] K. Rabaey, N. Boon, S.D. Siciliano, W. Verstraete, M. Verhaege, Biofuel Cells Select for Microbial Consortia That Self-Mediate Electron Transfer Biofuel Cells Select for Microbial Consortia That Self-Mediate Electron Transfer, *Applied and Environmental Microbiology*. 70 (2004) 5373-5382.
- [77] Z. He, F. Mansfeld, Exploring the use of electrochemical impedance spectroscopy (EIS) in microbial fuel cell studies, *Energy & Environmental Science*. 5692 (2009) 215–219.
- [78] A. Lamberti, N. Garino, A. Sacco, S. Bianco, D. Manfredi, C. Gerbaldi, Vertically aligned TiO<sub>2</sub> nanotube array for high rate Li-based micro-battery anodes with improved durability, *Electrochimica Acta*. 102 (2013) 233–239.
- [79] A. Tremouli, G. Antonopoulou, S. Bebelis, G. Lyberatos, Operation and characterization of a microbial fuel cell fed with pretreated cheese whey at different organic loads, *Bioresource Technology*. 131 (2013) 380–389.
- [80] Y. Qiao, S. Bao, C.M. Li, X. Cui, Z. Lu, J. Guo, Nanostructured Polyaniline / Titanium Fuel Cells, *ACS Nano*. 2 (2008) 113–119.
- [81] J. Menicucci, H. Beyenal, E. Marsili, G. Demir, Z. Lewandowski, Procedure for Determining Maximum Sustainable Power Generated by Microbial Fuel Cells, *Environmental Science & Technology*. 40 (2006) 1062–1068.



## Figure Captions

**Figure 1:** Schematic view (a) and picture (b) of the experimental set-up. In (b), from left to right there are the multi-channel syringe pump, an MFC, the anode and cathode recirculation vessels and the storage vessel; behind the MFC the multi-channel peristaltic pump is visible.

**Figure 2:** Equivalent circuit exploited for the fitting of the impedance spectra of Microbial Fuel Cells.

**Figure 3:** (a) Image of carbon felt, (b,c) FESEM images of carbon felt, (d) image of carbon-coated Berl saddles and (e,f) FESEM images of graphitized Berl saddles.

**Figure 4:** Quantification in gene copies/mL of planktonic samples from Carbon felt (a) and graphitized Berl saddles MFCs (b) for each strain by each probe during the time (logarithmic scale) on the top, and relative percentage values in the tables below.

**Figure 5:** Polarization curve (a) and power density (b) for the MFCs with Carbon Felt and Berl Saddles as anode electrodes, at initial time, and at 10 and 17 days running test.

**Figure 6:** EIS spectra of MFC based on carbon felt (a) and carbon-coated Berl saddles (b) anodes at 10-days running test. The points are experimental data and the continuous lines are fitting curves. The inset shows the high frequency region at larger magnification. (c) Charge transfer times at cathode and anode in MFC with carbon felt and graphitized Berl saddles as anode electrode, evaluated from EIS analysis.

**Figure 7:** Polarization curve (a), power density (b) and EIS spectra (c) of MFCs based on carbon-coated Berl Saddles anode before and after the refill operation. In (c) the points are experimental data, the continuous lines are fitting curves.

**Figure 8:** Voltage and power monitoring under external load in MFC with carbon felt and graphitized Berl saddles. The arrows indicate fed-batch of nutrients and change of cathode solutions.

Figure 1

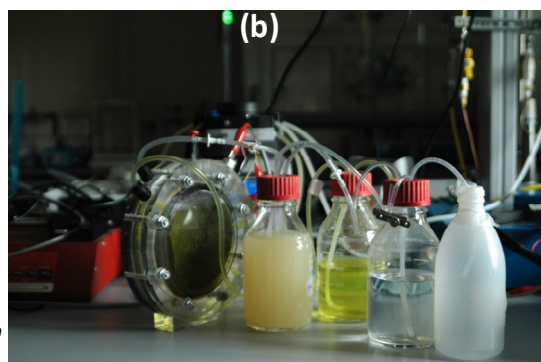
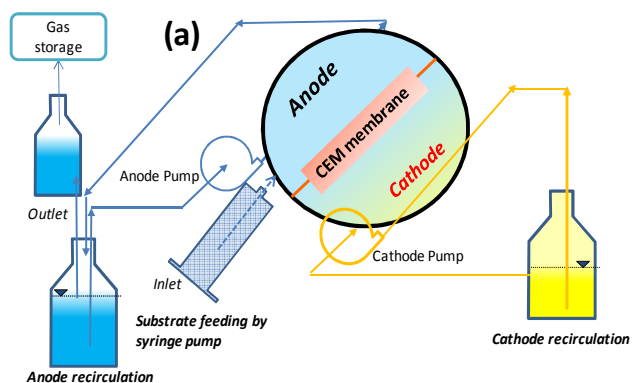
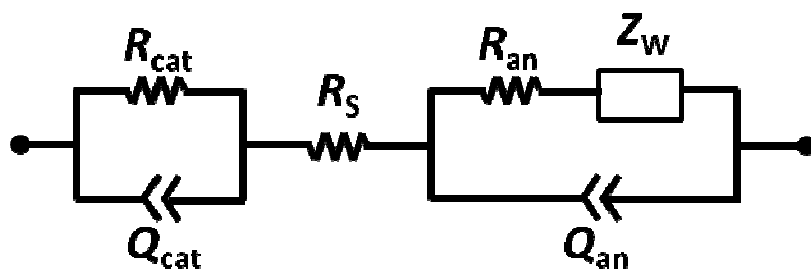


Figure 2



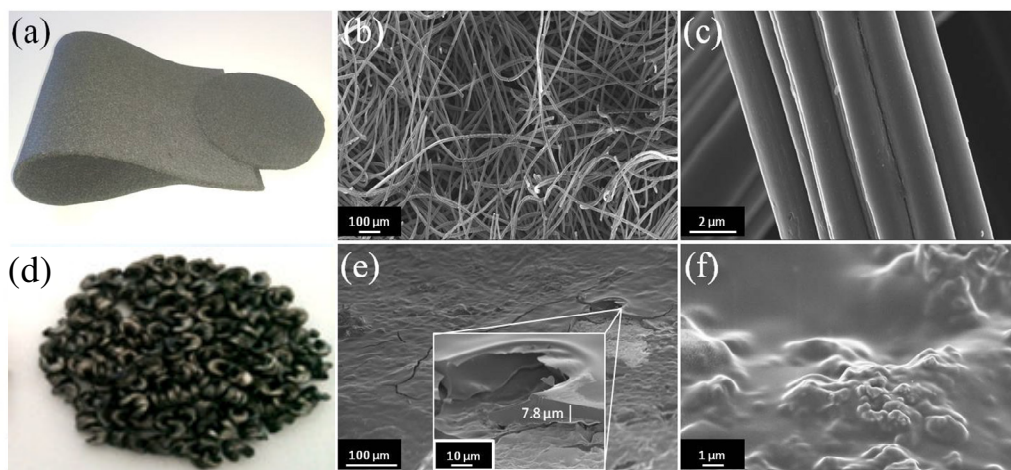
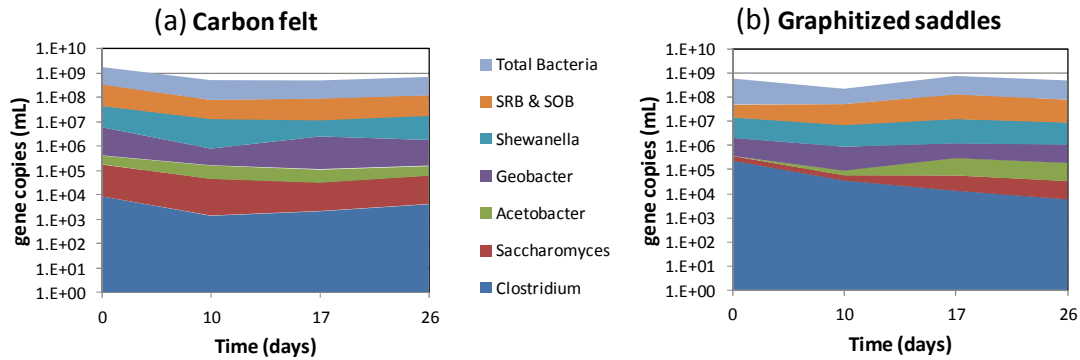
**Figure 3**

Figure 4



Carbon felt					
Relative percentage of microorganisms (%)					
SRB & SOB	20.892	15.154	19.313	18.080	
Shewanella	2.7030	2.9122	2.3226	2.8072	
Geobacter	0.3856	0.1412	0.5840	0.2744	
Acetobacter	0.0160	0.0259	0.0188	0.0155	
Saccharomyces	0.0119	0.0104	0.0076	0.0102	
Clostridium	0.0006	0.0003	0.0005	0.0007	
Time (days)	0	10	17	26	

Graphitized saddles					
Relative percentage of microorganisms (%)					
SRB & SOB	5.755	25.025	17.245	16.196	
Shewanella	2.217	3.654	1.690	1.851	
Geobacter	0.292	0.458	0.137	0.205	
Acetobacter	n.a.	0.020	0.036	0.037	
Saccharomyces	0.024	0.013	0.007	0.006	
Clostridium	0.040	0.020	0.002	0.001	
Time (days)	0	10	17	26	

Figure 5

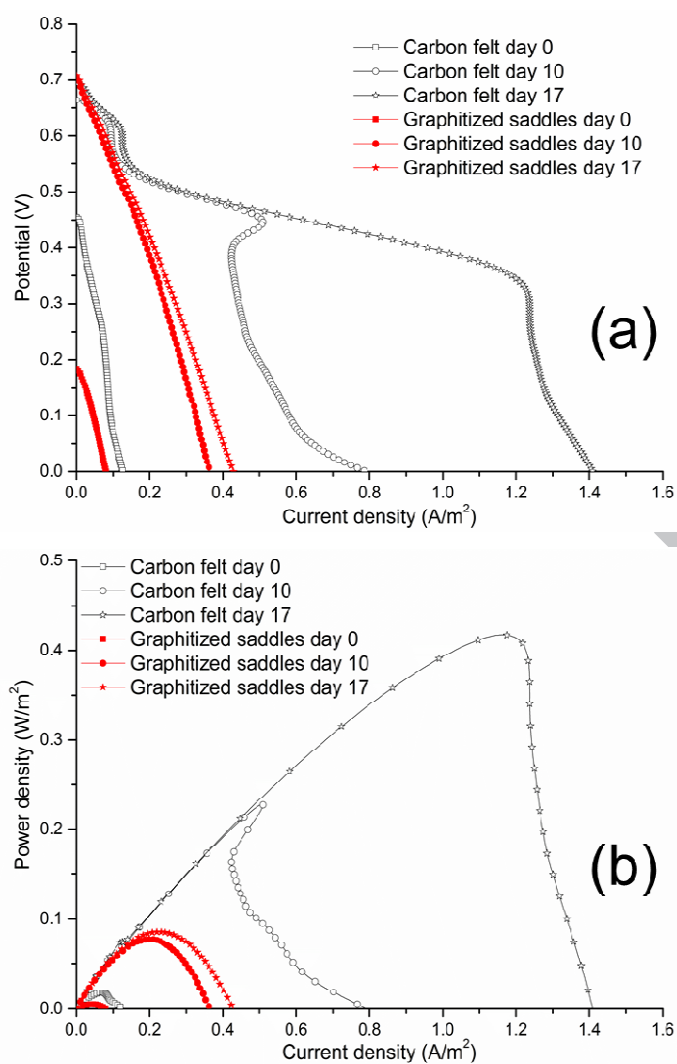


Figura 6

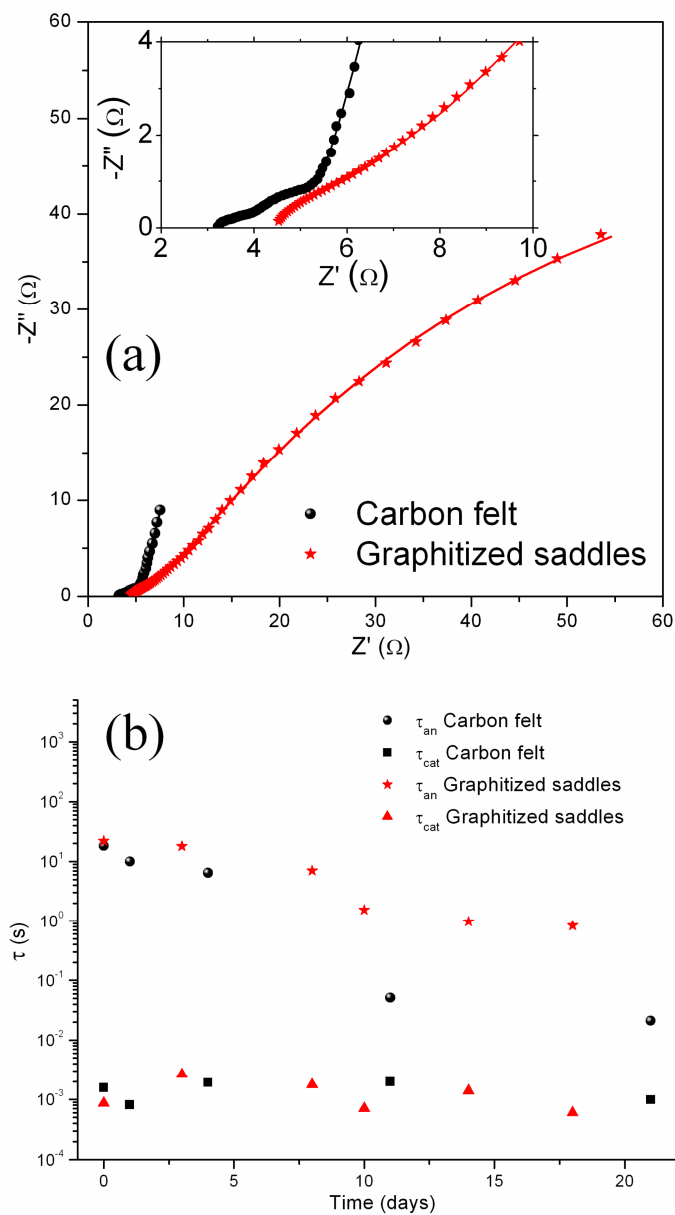


Figure 7

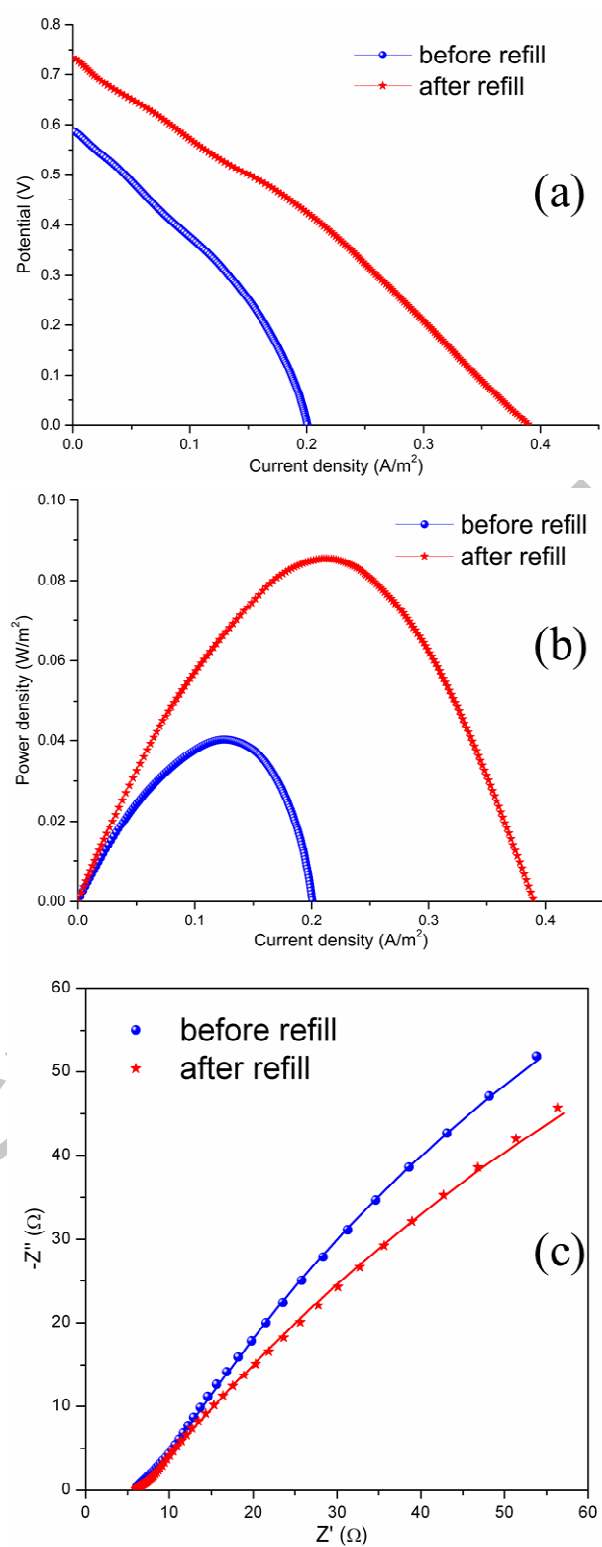
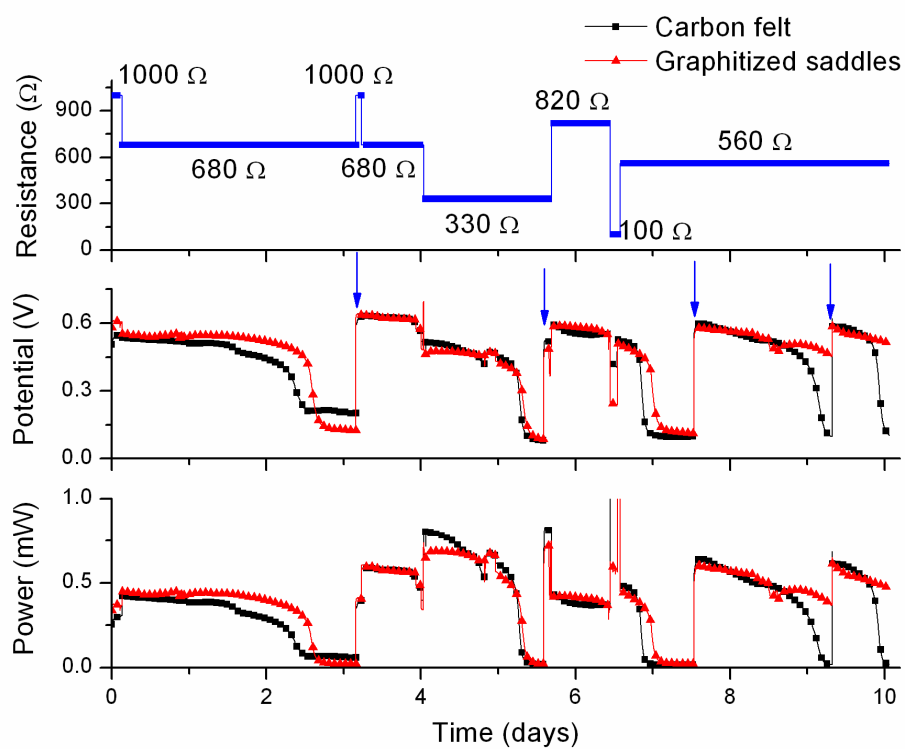




Figure 8



**Table Captions**

**Table I:** Microorganisms, Primers, Genomic Standards and total number of bases in the genomic DNA (bp), genes and number of copies of gene in  $\mu\text{L}$  of solution, tested in MFC biological analysis.

**Table II:** Characterization of MFCs after 10 days (stationary conditions), in terms of maximum power density  $P_{\max}$  and Internal Resistances calculated by Current Interrupt method ( $R_{\Omega}$ ) and by EIS.

**Table III:** Characterization of saddle-based MFC before and after refill in anode chamber, in terms of maximum power density  $P_{\max}$  and Internal Resistances calculated by Current Interrupt method ( $R_{\Omega}$ ) and by EIS.

Table I

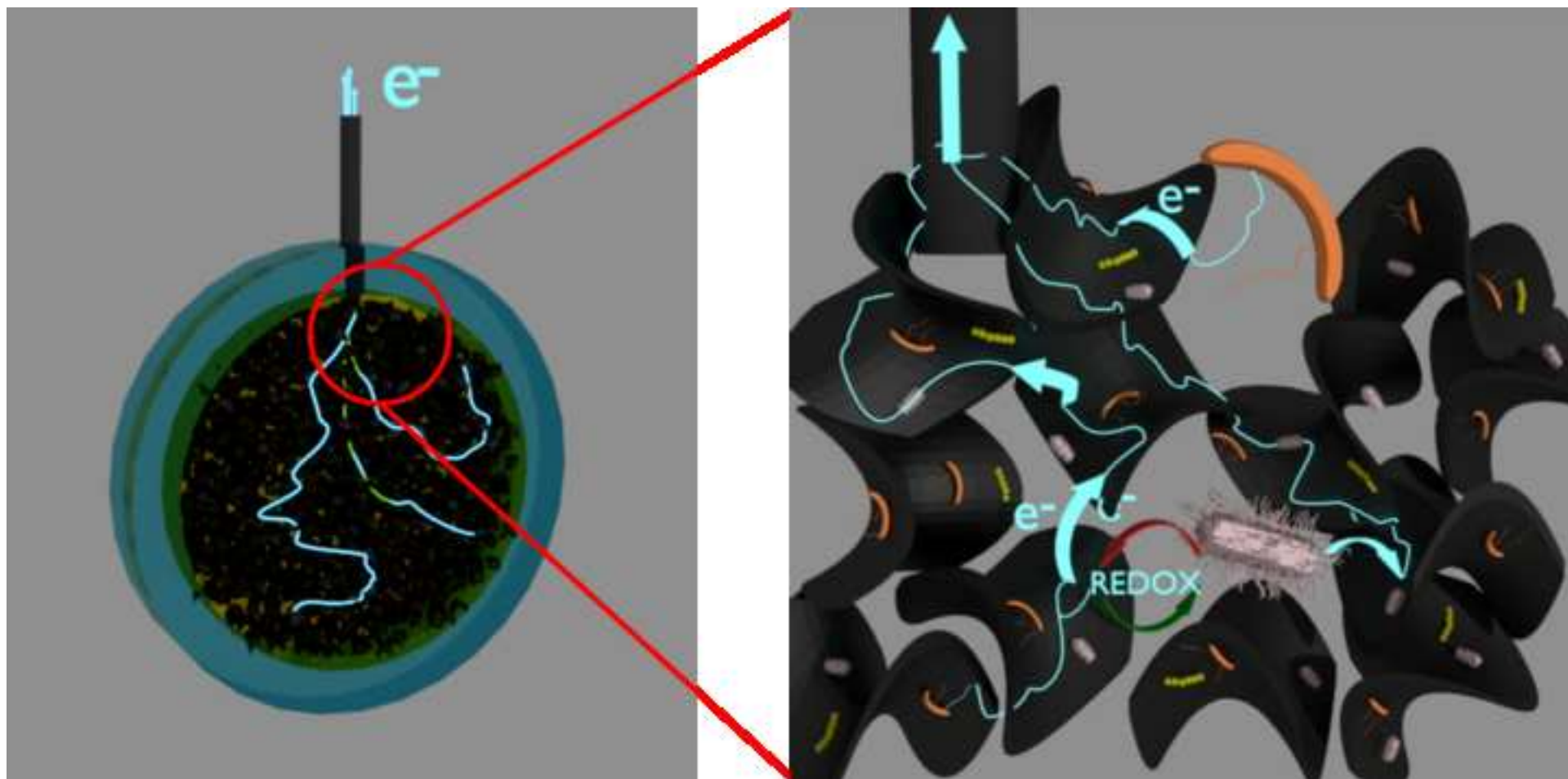
Microorganism	Primer name (gene target)	Primer (5' --> 3')	Genomic Standard (ATCC code)	Gene pb	Ref.
<i>Acetobacter</i>	Ace F	CGCAAGGGACCTCTAACACA	<i>Acetobacter diazotrophicus</i> (49037D-5)	110	[55]
	Ace R	ACCTGATGGCAACTAAAGATAGGG			
<i>Total Bacteria</i>	16S RNA F	AGAGTTTGATCMTGGCTCAG	<i>Desulfovibrio vulgaris</i> (29579D-5)	About 600	[56]
	16S RNA R	TTACCGCGGCKGCTGGCAC			
	probe	CCAKACTCCTACGGGAGGCAGCAG			
<i>Clostridium</i>	Clo F	ATTAGGAGGAACACCAAGTTG	<i>Clostridium difficile</i> (9689D-5)	307	[57]
	Clo R	AGGAGATGTCATTGGGATGT			
<i>Geobacter</i>	Geo F	AAGCGTTGTTGTCGGAATTAT	<i>Geobacter metallireducens</i> (53774D-5)	313	[58]
	Geo R	GGCACTGCAGGGGTCAATA			
<i>Saccharomyces</i>	Sac F	GCGGTAATTCCAGCTCCAATAG	<i>Saccharomyces cerevisiae</i> (9763D)	151	[55]
	Sac R	GCCACAAGGACTCAAGGTTAG			
<i>Shewanella</i>	She F	GCCTAGGGATCTGCCAGTCG	<i>Shewanella oneidensis</i> (700550D)	108	[59]
	She R	CTAGGTTTCATCCAATCGCG			
<i>Total Sulfate Oxidizing and Reducing Bacteria</i>	AprA F	GGGYCTKTCCGCYATCAAYAC	<i>Desulfovibrio vulgaris</i> (29579D-5)	About 300	[60-63]

Table II

MFCs	P <sub>max</sub> (mW/cm <sup>2</sup> )	R <sub>Ω</sub> (Ω)	R <sub>s</sub> (Ω)	R <sub>an</sub> (Ω)	R <sub>cat</sub> (Ω)	Z <sub>w</sub> (Ω/Vs)
<i>Carbon felt</i>	0.23	8	3.2	1.3	0.9	50.2
<i>Graphitized saddles</i>	0.08	20	4.3	162.8	4.1	---

Table III

MFCs	$P_{\max}$ (mW/cm <sup>2</sup> )	$R_{\Omega}$ ( $\Omega$ )	$R_s$ ( $\Omega$ )	$R_{an}$ ( $\Omega$ )	$R_{cat}$ ( $\Omega$ )
<i>Before refill</i>	0.04	18	5.9	362.5	2.7
<i>After refill</i>	0.09	16	5.8	287.2	2.6



## Dynamical analysis of Microbial Fuel Cells based on planar and 3D-packed anodes

### HIGHLIGHTS

1. Comparison of performances of two anode configurations, planar and 3D-packed
2. Berl saddles were covered by a graphite layer and used as packed electrode
3. Microbial consortia coming from sea-water used to catalyze biological oxidation
4. RT-qPCR protocol detects the presence of electrogens as *Shewanella* and *Geobacter*
5. Graphitized saddles satisfy electrical requirements and promote bacterial adhesion